



THE EFFECT OF RESTRICTION ON LIGHT-WEIGHT, LOAD-BEARING STEEL-CONCRETE COMPOSITE WALL PANELS BENEATH COMPRESSION

Priyanka bharati, M. Tech Scholar, Department of Civil Engineering, Faculty of Engineering & Technology, Rama University, Kanpur, India

Email Id: pri101292@gmail.com

Satish Parihar, Associate Professor, Department of Civil Engineering, Faculty of Engineering & Technology, Rama University, Kanpur, India

Email Id: satishparihar.fet@ramauniversity.ac.in

Abstract:

The strength of a mixed wall panel relies on its basic concrete endurance, level of solitary confinement as well as the combined action of the concrete and steel components. This article outlines an experimental research on how confinement impacts the axial capacity and behaviour of steel-foamed concrete composite panels. Five small-scale load tests are conducted on wall panels with varying stud configurations and sheet edge boundary conditions. Lightweight foamed concrete (LFC) serves as infill material, and the connection between the sheeting and concrete is established by using through-through studs. The load is mostly spread out throughout the concrete surface to prevent premature or brittle localised buckling of the sheet due to direct compressive loading of the wall panel. Vertical separation with diagonal shear failure of concrete are detected as failure mechanisms. The axial resistance of the wall is shown to rise in correlation with the level of confinement offered by fasteners and sheet edge conditions. The controlled lateral deformations of restricted concrete by steel sheeting, owing to interconnected studs, showed ductile deformations after reaching the peak behaviour. A novel approach is suggested to calculate the axial resistance of composite walls based on the failure modes identified during testing.

Keywords: panels made of steel and concrete composite, confinement measure, axial load capability thin-layer foamed concrete, Profiled sheets made by cold form

Introduction

Sheet-concrete composite walls consist of vertically aligned profiled sheets of steel with infill concrete and are a natural progression from composite floor panels used globally. Steel components are thin and susceptible to buckling, whereas the concrete infill offers resistance against buckling and thermal insulation at high temperatures. Figure 1 displays the schematic diagram of composite wall panels. Composite wall panels provide several benefits when combined with composite floor panels and may serve as core walls in steel frame building constructions, with the possibility for application in load-bearing construction. These panels may be used as a substitute for load-bearing brick walls, allowing for the construction of low-rise structures employing lightweight wall panels. Wright and Gallocher [1] examined the behaviour of composite wall panels throughout construction and service loading phases via a series of pilot experiments. The research emphasised the unique challenges present in non-traditional reinforced concrete construction. It was observed that the performance of wall panels is influenced by the bond strength between steel and concrete and the local buckling capacity of profiled steel sheets. Howard Wright conducted thirteen full-scale experiments to study the axial load behaviour of composite wall panels. The testing included various configurations of decking profile sheet types, test features, and loading circumstances. The tests revealed that the maximum yield stress in steel and concrete was not reached because of buckling in the thin steel component plates and the concrete's profiled form cross-section's inability to withstand eccentric moments resulting from flaws in the specimen and loading alignment. A proposal was made to adjust the frequently used squash load design formula by including plate buckling theory for steel and an empirical model for concrete, resulting in improved agreement with experimental data. Howard Wright [3] researched the axial and combined axial and bending behaviour of composite wall panels. The investigation was conducted on profiled steel sheets used in composite deck building. It was proposed that purpose-designed profiled steel

sheets may help composite wall panels reach the same structural efficiency as traditional reinforced walls. Anwar Hossain [4] investigated the possible use of composite wall panels as shear or core walls in structures, enabling apertures for doors and windows. The walls' strength was assessed based on established regulations and design formulas to provide design standards. Uy et al. [5] examined the combined axial and flexural strength of profiled composite wall panels using profile sheets manufactured in Australia. The trials were effectively used to calibrate a numerical model that included the impacts of local buckling. Mydin and Wang [6] examined the structural behaviour of lightweight steel-foamed concrete composite wall panels under compression. A feasibility study was carried out to showcase the suitability and constraints of composite wall panels in low-rise construction.

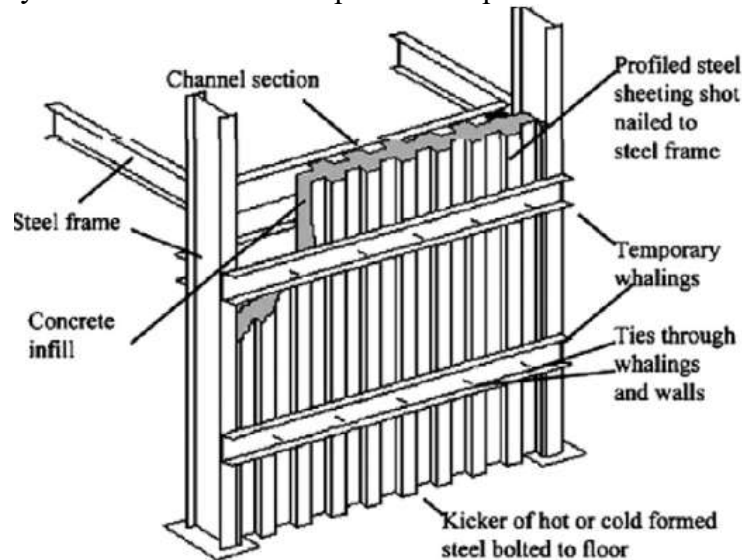


Fig. 1. Steel-concrete composite wall panel

The recommended panel has been determined to possess enough load-bearing capability for use in low-rise domestic construction of a maximum of four stories.

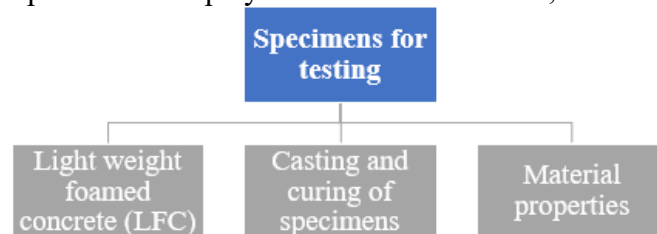
Previous research has shown that effective load transfer mechanisms, such as embossments or electromechanical relationships, are essential for optimising composite action and enhancing the performance of wall panels. The axial capacity of the wall panel is significantly affected by the early local buckling of steel sheets. In the experiments described in the literature, steel and concrete are evenly loaded together. Direct compression loading of steel sheet leads to early local buckling and diminishes the wall panel performance in the post-peak range. The current research seeks to analyse the basic characteristics of load-bearing composite wall panels constructed from steel that has been cold-formed and ultralight foamed concrete. The panels will be tested under axial compression stress with various connecting device arrangements. Compression loading is typically applied to the concrete part to analyse how the exterior steel sheets and interconnecting studs affect the load-deformation behaviours of the the panelled wall.

Specimens for testing

Four specimens have been identified. There are a total of five composite wall panellist specimens and two profiled LFC panels out of a total of seven examples. Figures 2 and 3 provide the configurations of the profile sheet and the wall dimensions, respectively.

The profile sheet has a thickness of 0.8 mm. The wall panel is 870 mm in height, 685 mm in width, and 130 mm in thickness. All examples fall into the short wall group with a slenderness ratio of 6.7, and failure is anticipated to be controlled by cross-sectional capacity. 8 mm diameter mild steel studs with a yield strength of 250 MPa are used for interconnecting sheets, tapering down to 7 mm at the ends. The tapered ends of the studs prevent the sheets from moving inward and facilitate the simple assembly of the specimens. The dimensions of the profile and wall are consistent across all specimens.

The aforesaid parameters are kept constant, while only the interconnection pattern and edge conditions are altered in the five composite wall panel specimens. The steel sheets have two edge the circumstances: unconfined edge, where the steel does not cover the concrete thickness, and completely confined edge, where channels are tack welded at both edges. Figure 4 displays the overall layout of the specimens, whereas Figure 5 shows the manufactured test specimens. The first three specimens (Specimen i.d. 1, 2, 3) out of five do not have restricted edges at the ends and are connected by 8 mm through-studs. Specimen 1 has two studs in the broader plate width area and is linked utilising a total of 30 studs throughout the height. The studs are spaced 72 mm apart horizontally and 200 mm apart vertically. Specimen 2 resembles specimen 1, with the exception of the central trough part without any connection. There are a total of 20 studs available. Specimen 3 is attached using 32 studs on the narrower plate width section, spaced 114.3 mm apart vertically. Specimen 4 features channels of dimensions 60×63×1.5 mm tack welded on both sides to serve as confined edges. It is linked using 6 studs in the smaller plate width section at the top, middle, and bottom of the panel. The studs are spaced 400 mm apart vertically. Specimen 5 displays restricted boundaries, but lacks any more connections.



2.1 Light weight foamed concrete (LFC)

The primary function of the infill concrete in composite panels is to prevent the sheets from bowing inward. LFC is a kind of porous concrete that is made by mechanically combining foam (pre-made, 0.1–1.0 mm-sized bubbles) with a cement-sand matrix-based concrete mixture. A unique piece of machinery known as a foam generator is used to create foam, which is then combined with a particular mixer. Foam dosage may be adjusted to obtain a density range of 200–1600 kg/m³, which is suitable for use as an insulating, structural, and partition material. As may be seen from the literature, brittle failure is the main drawback of LFC. LFC might be used in composite action with steel, which has great ductility, in load-bearing structure. For the purposes of this investigation, LFC with a density of 1200 kg/m³ has been chosen as the infill material. Foam is made by a protein-based compound called rheo-cell. A kilogramme of chemical yields 660 litres of foam. The cement used is Ordinary Portland Cement (OPC) of 53 grade that complies with IS: 12269 [7]. Fly ash is another supplementary cementations material used in addition to cement. For LFC, fine sand that satisfies IS: 383 [8] and passes through a 1.18 mm screen is used to provide foam stability and strong flow properties. The ratios of cement to sand (1:0.87) and water to binder (0.39) are maintained.

2.2 Casting and curing of specimens

A wooden board supports the wall panel specimens for themselves, and a spirit level is used to examine the levels. In order to prevent specimens from bulging from the pressure of the concrete, shuttering is positioned all the way along the specimen.

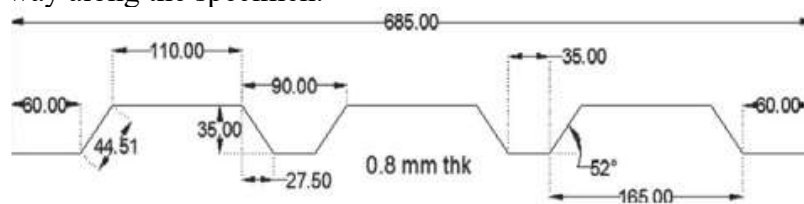


Fig. 2. Profile sheet configurations

In order to avoid any localised concrete crushing during loading, a steel wire mesh is cut to the form of the profile and maintained 35 mm below the top and bottom levels of the specimen during casting. Fig. 6 depicts the wire mesh's location.

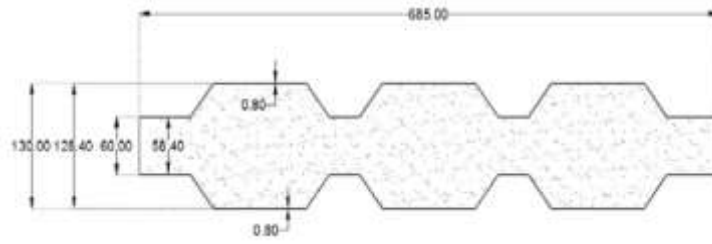


Fig. 3. Wall dimensions.

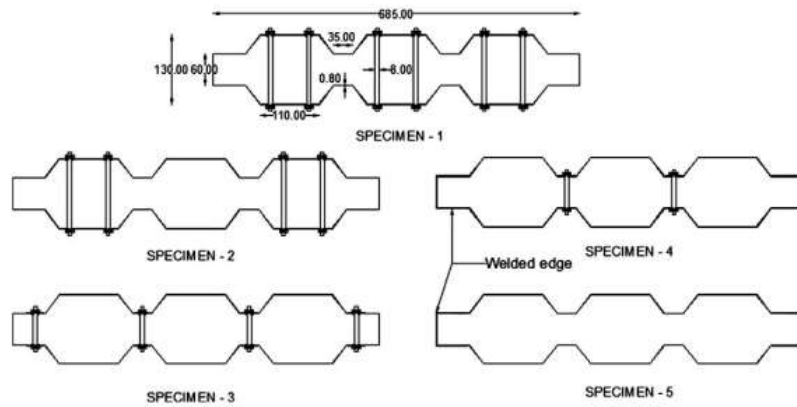


Fig. 4. General arrangements of specimens.

Furthermore, to investigate the contribution of LFC core to the strength, two sets of foam concrete profiled panels (ID PP1 and PP2) without steel sheets are also cast. Fig. 7 depicts the LFC specimens.

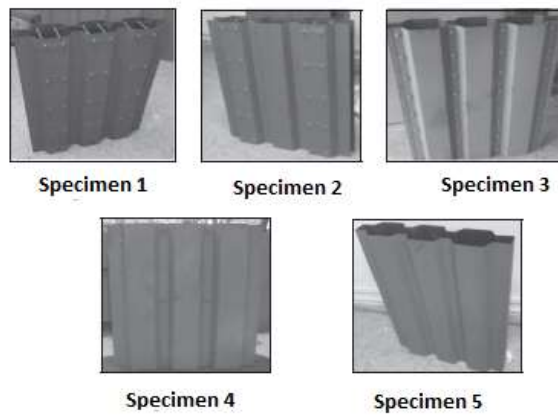


Fig. 5. Test specimens.

The vertical casting of LFC panels corresponds to the loading direction. Polythene sheets are used to encapsulate the test samples, which are then allowed to self-cure for 28 days by reusing the water vapour that evaporates as a result of heat-induced hydration.

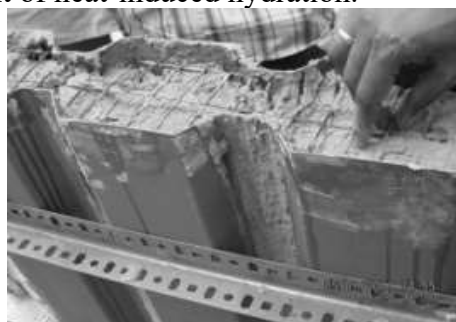


Fig. 6. Position of steel wire mesh.

On the same day as the composite panel casting, LFC cubes and cylinders are cast. On the eightieth day after casting, tests are conducted on the LFC and wall panels to verify that the metallic action of fly ash has fully developed in terms of durability.

2.3. The material the characteristics

In order to assess the material qualities of cold produced sheet, three pressure coupon specimens are created from the same batch of sheets as the test specimens. Figure 8 shows the stress-strain curve of the sheet. Table 1 shows the material parameters of the sheet acquired during the coupon test. The sheet's average yield and ultimate stress are 261.3 and 363.8 MPa, respectively, with a Young's modulus of 2×10^5 MPa. Each batch of concrete involves the casting of six cubes and cylinders. The cubes (100×100×100 mm) and cylinders (100 mm dia, 200 mm length) are tested on the same day as the wall panelling (78 days).



Fig. 7. Foamed concrete panel.

The compressometer is made up of two linear variable differential transducers (LVDT 1 and LVDT 2) that monitor the average axial deformation and strain of concrete cylinders to determine modulus of elasticity. Figure 9 shows the stress-strain behaviour of a typical foam concrete cylinder. A maximum compressive strain of 0.002 was found.

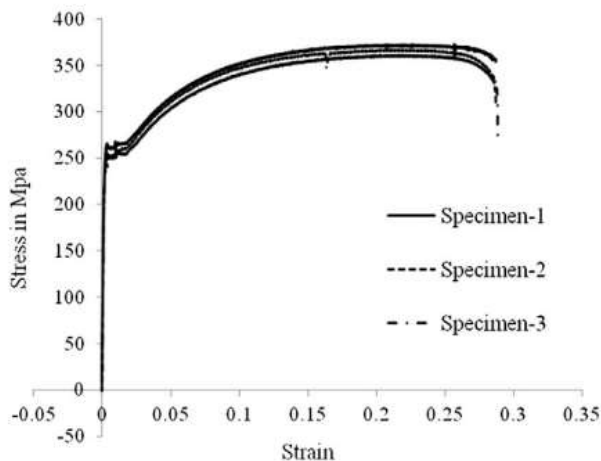


Fig. 8. Stress–strain behaviour of steel sheet.

Table 1 Properties of cold formed steel sheet.

Specimen no.	Thickness (mm)	Young's modulus E (MPa)	Yield strength fy (MPa)	Ultimate strength fu (MPa)	% Elongation
Specimen 1	0.8	200,000	261.5	359.4	27

Specimen 2	0.8	200,000	270.6	365	28
Specimen 3	0.8	180,000	251.8	367	29

The substance parameters of LFC are shown in Table 2. The typical compressive strengths of the cube and cylinder at the 80th day is 7.9 MPa and 6.8 MPa, accordingly The Young's modulus, which is the value for LFC is 4633 MPa, which stands

3.0 The experimental examinations

The primary goal of experimental research is to assess how confining impacts the performance of wall panel systems loaded under axial compression. A total of five composite wall panels and two LFC panels were evaluated. The tests were conducted using a servo-controlled Universal Testing Machine (UTM) with a maximum capacity of 250 tonnes. Figure 10 displays the schematic diagram of the test set-up. A hardwood board and steel plate, each measuring 700 mm in length, 150 mm in width, and 30 mm in thickness, are positioned above and below the specimen.

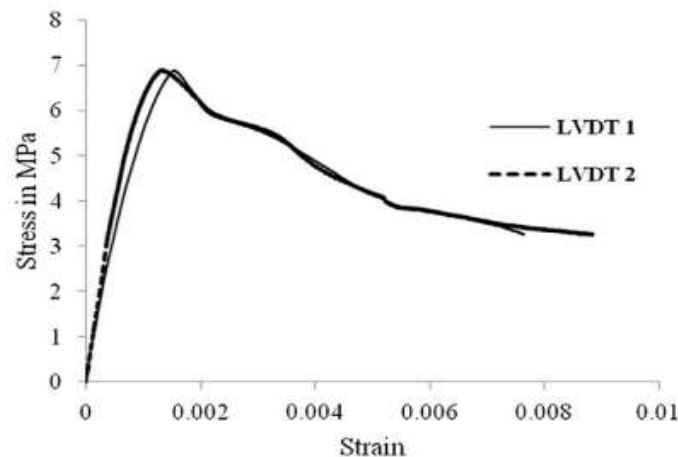


Fig. 9. Stress–strain behavior of LFC cylinder.

Plaster of Paris is used to guarantee the connection between matching surfaces. Directly loading steel sheets beneath compression causes early local buckling. To counteract this, a deformable wooden board made of soft material is placed on top of the test piece using plaster of Paris. The hardwood plank equally distributes the stress on the hardened concrete surface after being punctured by the steel sheet edges. A heavily reinforced distributor I-beam is positioned above the steel plate to evenly distribute the weight throughout the wall's breadth. The system is designed such that the centre of gravity of the test setup aligns with the centre of loading point of the UTM, as seen in Figure 11. Dial gauges are positioned on both sides of the specimen in the centre to measure the centre lateral deflection of the sheet. One LVDT is positioned on the exposed concrete surface and another LVDT is put on the sheet to measure axial deformation. Six strain gauges are affixed to each specimen along the height in the central trough section to measure the strain response of the sheet. An axial compression load is delivered at a rate of 0.5 mm/min in a displacement-controlled manner. The identification of the specimens may be found in Table 3.

Failure of test specimens

Fig. 12 displays the modes of failure for every test specimen. The LFC panels failed suddenly with a brittle fracture mechanism under axial loading. LFC panels exhibit the vertical splitting crack pattern (I.D. PP1 and PP2). According to the LFC panels' failure mode, a vertical splitting failure can be avoided by using bolts or studs to provide some sort of interconnection. The hardwood plank evenly distributes the initial load to the concrete and steel.

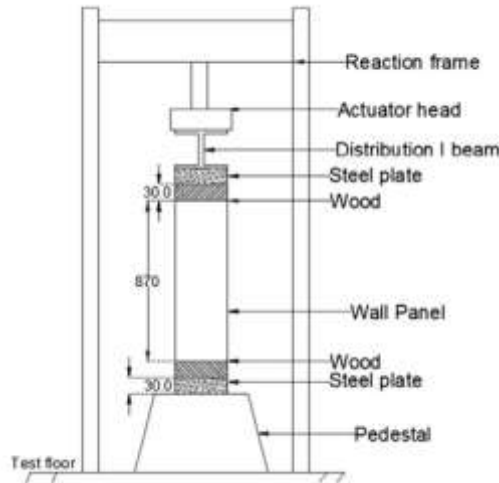


Fig. 10. Schematic arrangement of test set-up for wall panel.

Following the deformation of wooden planks by the edges of steel sheets, the weight is evenly distributed to the concrete part alone, applying lateral pressure to the steel sheets. The uncovered sides of specimens without limited edges show the vertical displacement of the titanium sheet's external flange panel from the substrate.

Specimen	F _{ck}	F _{cy}	Modulus of elasticity, E (MPa)
	Mpa (78 days)		
	Cube	Cylinder	
Batch 1	8.3	6.9	5000
Batch 2	7.3	6.7	4000
Batch 3	8.0	6.9	4900

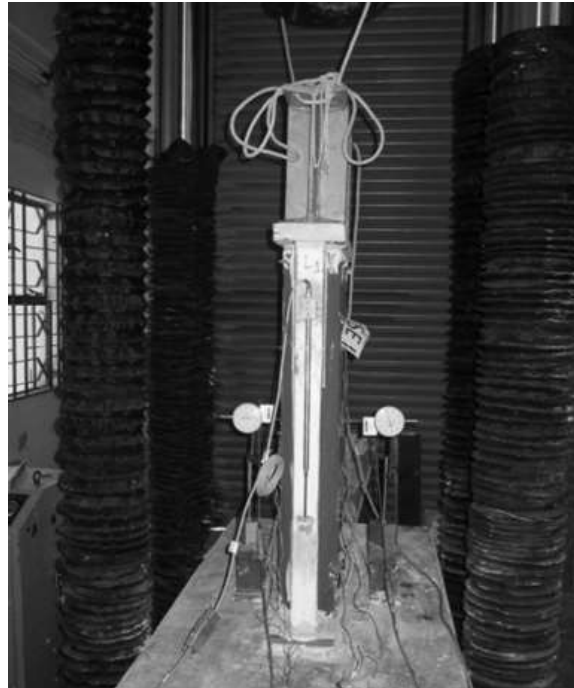


Fig. 11. Instrumentation of wall panel

On the wall's sides, diagonal shear cracks and coupled vertical separation were caused by the direct stress of the concrete surface. Localized bending of the steel sheets close to the crack and localized crippling of the sheets along the wall's breadth perpendicular to the crack were produced by the load shifting from the cracked concrete to the steel sheet. The first three species with unconfined edges

exhibit the failure type described above. In specimen 1, a diagonal tension shear crack is visible above the specimen's bottom row of connecting studs. The diagonal compression shear crack that started at the top corners of the wall panel beneath the first and second row of connecting studs is what caused specimens 2 and 3 to collapse similarly to specimen 1. In specimen 4, the top, middle, and bottom portions of the wall are equipped with six studs (a smaller trapezoidal part) and two welded channels that are tack welded to the sheet for complete confinement. Steel sheets began to bulge between connecting studs as a result of the vertical separation and crushing of the concrete, which also attempted to open up the re-entrant corners of the sheet. Along the studs in the breadth direction, local crippling of the sheets is also seen. The failure mechanism for specimen 5, which has completely restricted edges and no stud connections, is vertical concrete separation and crushing.

Table 3 Specimen I.D.

Wall panel specimens	Foam concrete specimens
Specimen 1	PP 1
Specimen 2	PP 2
Specimen 3	
Specimen 4	
Specimen 5	

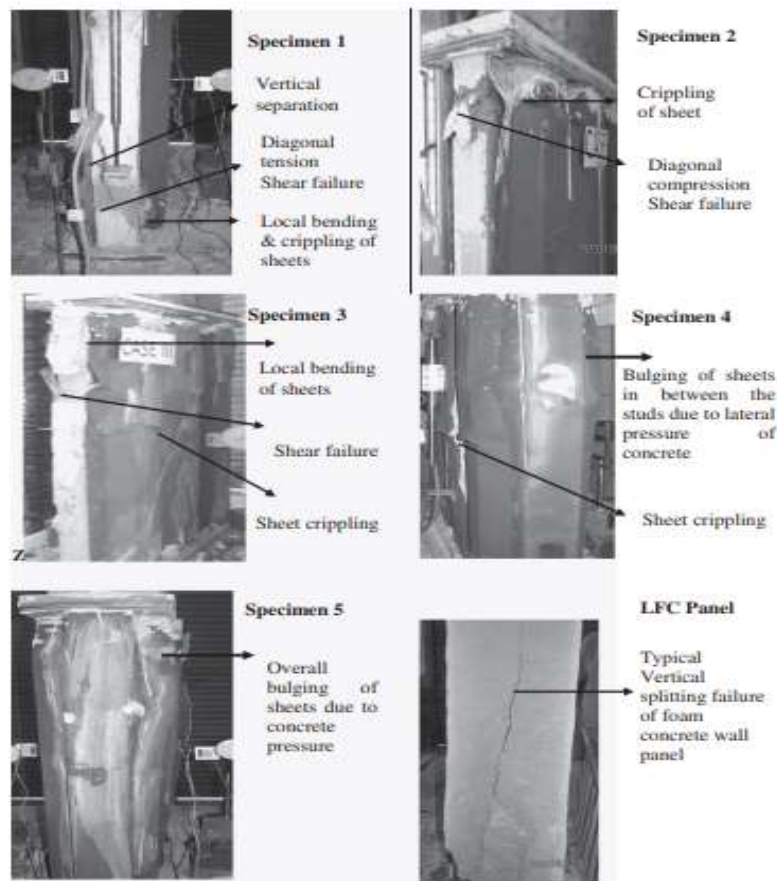


Fig. 12. Failure of test specimens.

3.2. Load-deformation response of test specimens

Figure 13 displays the relationship between axial load and total deflection for wall panel specimens and the foam concrete specimen (PP2). The plot clearly shows that enclosing foam concrete with steel sheets on both sides and connecting studs allowed the panel to withstand greater loads and improve

ductility. All wall panel specimens exhibited a consistent trend/behavior. The LFC specimens did not exhibit the descending segment of load-deformation behavior because to their brittle breakdown. The initial decrease in the load signifies the collapse of foam concrete. Increasing loads break concrete, causing lateral pressure on the sheets. The containment of concrete by steel sheets and connecting studs allowed for an additional load almost equivalent to the initial peak load to be achieved. Studs prevented sheets from bulging outward due to lateral pressure, causing local damage along the studs and reducing load capacity after the second peak. Specimens 4 and 5 experienced outward bulging of sheets due to the lack of studs and low numbers present, resulting in increased lateral pressure from the concrete. Additional load led to the redistribution of weight to different areas, allowing all specimens to endure around 70% of the initial peak load while experiencing an increase in ductile deformations. The decrease in the load-deflection curve following the second peak is a result of the controlled lateral deformations of the confined concrete by the steel sheet due to the interconnecting studs. The concrete at the top and base of all examples was uncrushed, suggesting that the steel mesh placed at both edges successfully transferred the weight without causing local crushing failure. Table 4 displays the failure load of all specimens tested.

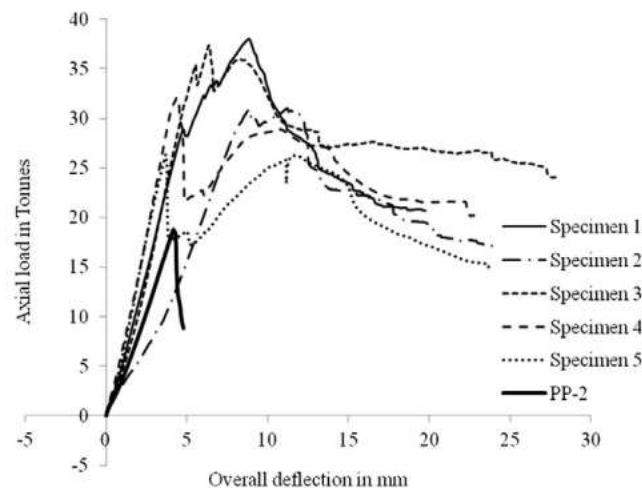


Fig. 13. Axial loads versus overall displacement response of specimens

The failure load of PP1 and PP2 specimens is 14.9 tons and 19.12 tons, respectively. Specimen 1 has the highest ultimate load capacity of 38.9 tons. Specimen 3 has a capacity of 37.8 tons, which is near the failure load of specimen 1. Specimens 1 and 3 have equal initial stiffness, however specimen 3 with studs in the outer flange plate maintained a larger post-peak load. Specimen 1 and 2 are very identical, with the only difference being the absence of studs in the middle trough part of specimen 2. Specimen 2 has a capacity of 31.4 tons and exhibits lower initial stiffness due to the absence of connections in the middle trough area. Specimen 4, which had welded edges and was attached using six studs, had a failure load of 32.5 tons when compared to specimen 5. Specimen 5 is akin to specimen 4, lacking interconnecting studs, with a failure load of 27 tons, 5.5 tons lower than specimen 4. Specimens 4 and 5 exhibit identical initial stiffness and post-peak behavior, differing only in the failure load. Therefore, the studs have helped bear the weight. examples 4 and 5, which have welded edges, exhibit a stiffer initial curve compared to examples 1, 2, and 3 without welded edges due to the complete confinement of concrete. The axial stiffness of a wall panel is influenced by the level of confinement pressure from studs and welded edges. The axial rigidity of a wall panel increases with both fully constrained edge conditions and a higher number of studs. Axial deformation during failure can be increased by 3 to 5 times compared to LFC specimens, and it occurs without rapid failure.

3.3. Load-strain response of test specimens

Strain gauges are attached to the central wider plate at different points along the wall panel on both sides. Fig. 14 displays the placement of strain gauges. All specimens reached an ultimate concrete strain of 0.002, indicating that the concrete reached its maximum load capacity under axial

compression. Figure 15 displays the typical load versus strain behavior of specimen 1. Figure 15's demarcation line indicates the force threshold for when steel sheet punching of wood occurs. The linear segment of the load-strain curve below the line signifies the even distribution of load on both steel and concrete. Above the line, only the concrete part is loaded, exerting lateral pressure on the sheet and creating tensile strain (S2-S6) in the sheet. The concrete's lateral pressure caused the sheet to swell, but the numerous studs in specimen 1 prevented outward bulging, leading to the sheet being crippled along the studs. Therefore, reduced strain values are noted at the final phase. Specimens 4 and 5 exhibited considerable outward bulging, resulting in slightly higher strain values of roughly 1000 μm during axial compression testing. Figure 15 displays the typical load versus strain behavior of specimen 1. Fig. 15's demarcation line indicates the load required for the steel sheet to punch through the wood. The linear segment of the load-strain curve below the line signifies the even distribution of load on both steel and concrete. Above the line, the concrete part is solely responsible for applying lateral pressure on the sheet, resulting in tensile strain (S2-S6) in the sheet. The concrete's lateral pressure caused the sheet to swell, but the numerous studs in specimen 1 prevented outward bulging, resulting in the sheet becoming crippled along the studs. Therefore, lower strain values are noted at the final stage. Specimens 4 and 5 exhibited substantial outward bulging, resulting in slightly higher strain values of around 1000 μm .

4. Composite material wall construction

The recommendations for construction in BS:8110, Eurocode 4, as well as AS:3600 consider that the axial capacity is the combined strength of steel and concrete, accounting for reduction factors due to potential compressive bending stresses from slight eccentric loading or initial imperfections, as well as reduced concrete strength. Past experiments showed that the axial load capacity is affected by local buckling of thin sheets and decreased area of concrete cross-section due to profiling. The codal equations do not include the impact of these two factors, leading to an overestimation of capabilities. Wright [12] suggested a precise technique to forecast the buckling capacity of plates in contact with concrete by determining stress limits for sections according to boundary circumstances. Wright [2] suggested a reduction factor to consider the void generated by profiling on the compressed border of the wall. Reduction factors were developed in the literature using experimental research to adjust for the above issues. Modified design equations were proposed, leading to more accurate capacity estimations compared to previous ones. The codal equations rely only on the area of steel sheet and concrete, resulting in consistent capacity estimations for specimens regardless of the number of studs or other mechanical linkages.

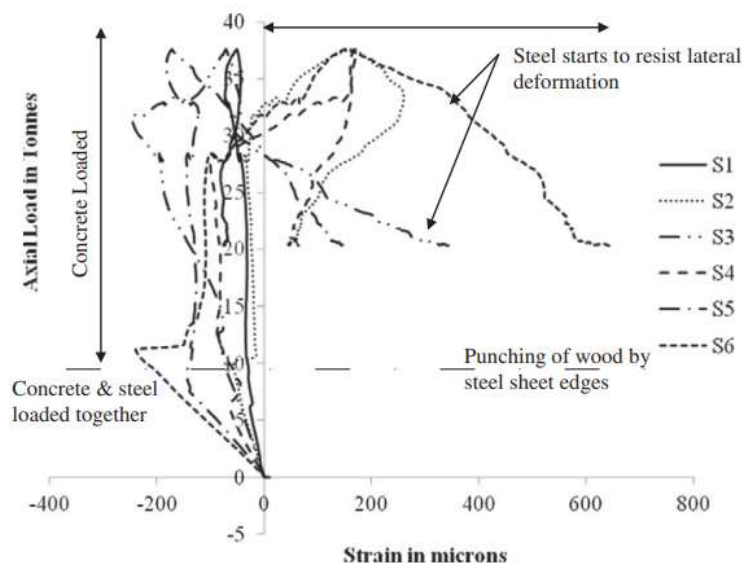


Fig. 15. Load versus strain behaviour of specimen 1.

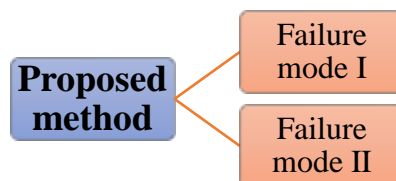
The tests clearly show that the axial strength of the wall panel is affected by the level of confinement provided by the studs and steel sheet. The maximum load-bearing ability of wall panel specimens is determined by the increased strength of concrete when confined. The confinement pressure changes based on the quantity of studs and the characteristics of the sheet edges. The sheet serves just as a barrier and does not enhance the strength. Therefore, it is not suitable to use the strength of the steel sheet when estimating the failure load. The steel sheet indirectly boosts the concrete's strength by providing confinement. A novel approach is suggested for estimating capacity using experimental observations and failure causes.

4.1. Proposed method

Concrete strength evaluation utilizes failure mechanisms. A novel technique is suggested for predicting the strength of wall panels by considering the failure processes.

Two failure mechanisms were discovered throughout the tests:

- ✚ Cracking of foam concrete in the upward direction
- ✚ Shear collapse of concrete towards the very top or bottom of a wall panel due to transverse contraction or tension.



4.1.1. Failure mode I

In this scenario, it may be assumed that all the steel along the failure plane is providing containment. The confining stress σ_c may be represented mathematically.

$$\sigma_c = \frac{A_{sc}f_y}{WH}$$

in the guise of nothingness

$$\frac{\sigma_c}{f_{ck}} = \left(\frac{100A_{sc}}{WH} \right) \left(\frac{f_y}{f_{ck}} \right)$$

4.1.2. Failure mode II

Shear failure may happen when the maximum tension surpasses the combined strength of the material and the stress applied by the steel sheets. During testing, it was noticed that the steel sheets flex over the top area of around 250 mm, indicating a failure. When there is a failure, the deformation may be simplified and represented as seen in Figure 17. The bending moment capacity for the complete width may be calculated by using the yielding of plates, resulting in a value of 1934 kNmm. This value can then be used to get the value of σ_{cb} , which is found to be 0.36 MPa. The axial tensile strength of concrete, f_t , may be determined by multiplying 0.3 times the characteristic compressive strength of concrete, f_{ck} , and the square root of the ratio of the effective prestress force, p . This calculation results in a value of 0.85 MPa. The axial stress σ_a may be determined by using the equation that ensues.

$$f_t = -\left(\frac{\sigma_a + \sigma_{cb}}{2}\right) + \sqrt{\left(\frac{\sigma_a - \sigma_{cb}}{2}\right)^2 + \tau^2}$$

5. Conclusions

This report outlines the experimental procedures used to examine the response of the structure of composite panels for walls under axial stress. The load is only applied to the concrete part in order to examine the impact of the confinement of concrete by the restricted edges and interconnected studs on the load deformation characteristics of the wall panel. The foam concrete specimens exhibited a sudden manner of failure characterized by brittle fracture. When examining the composite wall specimens with unconfined edges, we detect the occurrence of diagonal edge shear fractures, which may be either



tension or compression shearing cracks. Additionally, vertical splitting of the pavement is seen, followed by the crippling of the steel sheets. The failure mechanism of specimens 4 and 5, which have entirely constrained edges, is primarily determined by the vertical splitting and crushing of concrete in the middle section, followed by the general bulging of the steel sheet. The load bearing capability of all the wall panel specimens ranged from 27 to 38 tonnes, demonstrating good performance. The load bearing capability of panels for walls is seen to augment with the level of confinement offered by the studs and enhanced sheet edge conditions. These composite boards have an axial strength that is more than 200% higher compared to regular foam concrete panels. The restricted concrete experienced controlled lateral deformations caused by the steel sheet with interconnecting studs, resulting in ductile deformations after the post-peak behaviour. All codes assume complete interaction between steel and concrete, and the strength is measured by considering the strength of both materials. According to the current investigation, it has been determined that the steel sheet serves only to increase the strength of concrete via confinement, and does not directly contribute to its strength. The axial deformation at failure exhibits a significant increase, ranging from 3 to 5 times that of simple foam concrete specimens. Furthermore, the failure does not occur suddenly.

A novel approach is being suggested for predicting the strength of composite wall panels by taking into account the confinement effect, which is based on the causes of failure. The suggested technique provides a more accurate assessment of strength and demonstrates a strong association with the test findings. Wall panels containing infill lightweight foamed concrete exhibit notable axial load carrying capacity and ductile performance, making them suitable for load-bearing construction in low-rise structures. Further investigations are required to study the potential of the wall panels to function as shear walls, taking into consideration their ductile properties. These studies should be conducted under various loading circumstances. The composite wall panels has significant potential for improving seismic performance, retrofitting, impact resistance, and durability in shock-resistant requirements.

References

- [1]. Wright HD, Gallocher SC. The behaviour of composite walling under construction and service loading. *J Constr Steel Res* 1995;35:257-73.
- [2]. Wright Howard. The axial load behaviour of composite walling. *J Constr Steel Res* 1998;45(3):353-75.
- [3]. Wright Howard. Axial and bending behaviour of composite walls. *J Struct Eng* 1998;124:758-64.
- [4]. Anwar Hossain KM. Axial load behaviour of pierced profiled composite walls. *IPENZ Trans* 2000;27(1):1-7.
- [5]. Uy B, Wright HD, Bradford MA. Combined axial and flexural strength of profiled composite walls. *Proc Inst Civ Eng Struct Build* 2001;146(2):129-39.
- [6]. Mydin Md Azree Othuman, Wang YC. Structural performance of lightweight steel-foamed concrete steel composite walling system under compression. *Thin Walled Struct* 2011;49:66-76.
- [7]. Indian standard:12269–1987. Specification for 53 grade ordinary portland cement. New Delhi: Bureau of Indian Standards.
- [8]. Indian standard:383–1970. Specification for coarse and fine aggregates from natural sources for concrete. New Delhi: Bureau of Indian Standards.
- [9]. British Standards Institute:8110. Structural Use of Concrete. Code of practice for design and construction, Part I; 1985.
- [10]. Euro code 4, Design of composite steel concrete structures: Part 1.1. General Rules and Rules for Buildings, DD ENV 1994-1-1, London: BSI.
- [11]. AS: 3600. Standards Association of Australia, Concrete Structures; 1998.
- [12]. Wright HD. The buckling of plates in contact with a rigid medium. *Struct Eng* 1993;71:209-15.